# Optical MEMS and Nano-Photonics for Diagnostics

Aaron T. Ohta, Hsan-Yin Hsu, Arash Jamshidi, and Ming C. Wu
Dept. of Electrical Engineering & Computer Sciences
University of California, Berkeley
Berkeley, CA, USA
wu@eecs.berkeley.edu

***Abstract*—We present the capabilities of the optoelectronic tweezers device (OET) as related to medical diagnostics. OET is capable of single-cell manipulation and discrimination. Furthermore, nanoscale structures can be manipulated with OET to create sensors and probes.**

***Keywords-Optoelectronic tweezers; dielectrophoresis; nanowire manipulation***

## I. INTRODUCTION

Medical diagnostic techniques can be improved with manipulation and interrogation techniques at the single-cell level. Single-cell manipulation enables researchers to study cell-to-cell signaling and interactions, and can aid in drug screening and other assays. Diagnostics also benefits from improved sensor technology. Nanowire-based sensors offer high sensitivity, due to large surface area to volume ratios. In addition, nanowires can also be used as cellular probes, as in near-field scanning microscopy.

Current tools for single-cell manipulation include optical tweezers [1] and dielectrophoresis [2]. Optical tweezers uses the gradient force of a highly-focused laser to trap objects. Optical tweezers provides dynamic single-cell control, but has limitations for parallel manipulation. In addition, the optical energy can affect or damage the cells under manipulation [3].

Dielectrophoresis (DEP) is the low-frequency analog of optical tweezers. Dielectrophoretic force is induced when an induced dipole interacts with a non-uniform electric field. The electric fields are typically formed using microfabricated metal electrodes [2]. Thus, the manipulation patterns are not dynamic, and it can be difficult to simultaneously address objects on widely-varying length scales.

Our research group has developed a tool called optoelectronic tweezers (OET) that complements optical tweezers and DEP devices [4]. OET can manipulate microscale objects, such as single cells, as well as nanoscale objects, such as nanowires. In this manner, single-cell behavior can be studied, while nanoscale objects can be positioned to further probe cellular behavior.

Here, we present the operating principle of the OET device and potential applications in medical diagnostics. We demonstrate the OET capability of distinguishing between live and dead cells, and between different cell types. We also demonstrate cell manipulation in native cell culture media. Furthermore, we demonstrate OET manipulation of nanowires, which can be used to form sensors or cellular probes.

## II. OPTOELECTRONIC TWEEZERS

### A. Operating Principle

The OET device relies on optically-induced DEP to impart a force on the particles under manipulation. The DEP force is controlled by optical patterns that are projected on the photosensitive surface of the devices.

The optoelectronic tweezers device consists of two electrodes (Fig. 1). The upper planar electrode consists of a 100-nm-thick layer of indium-tin-oxide (ITO), a transparent conductive material, on a glass substrate. The lower photosensitive electrode consists of featureless layers of ITO and amorphous silicon (a-Si) on a glass substrate. The two electrodes form a fluidic chamber that is typically 100 μm in height. An aqueous solution containing the cells or particles under manipulation is introduced into the chamber, and an electric field is created in the device by applying an ac bias across the top and bottom electrodes.

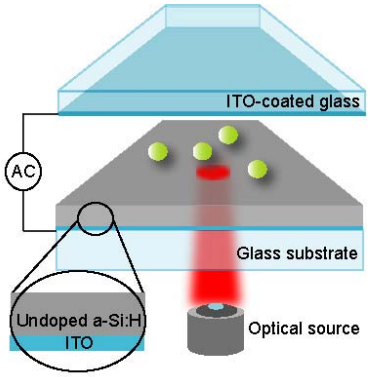


Figure 1. The OET device consists of a top transparent ITO electrode, and a bottom a-Si:H photosensitive electrode. A variety of optical sources, such as LEDs, halogen lamps, or lasers, are used to create dynamic optically-defined electrodes on the photosensitive surface

The a-Si film has its conductivity modulated by the intensity of the light that is absorbed in the material. Under ambient light and a 5V bias, the a-Si film has a conductivity of $0.9 \times 10^{-6}$ S/m. However, when illuminated with light, the conductivity of the a-Si layer increases by a few orders of magnitude, to $1.7 \times 10^{-2}$ S/m under an illumination intensity of 145 W/cm$^2$. The a-Si layer thus has two states; a low-conductivity dark state, and high-conductivity illuminated state. Furthermore, the transition between these two states is confined

978-1-4244-2879-3/08/$25.00 ©2008 IEEE

to the region under illumination, due to an ambipolar diffusion length of only 100 nm in amorphous silicon [5]. These two states allow the a-Si layer to act as an optically-controlled and optically-defined electrode. Thus, the voltage drop in the device is modulated between the a-Si layer (in the dark state) and the liquid layer (in the illuminated state). As a result, high electric fields are present in the illuminated areas, creating the electric field gradients necessary for DEP.

### *B. Dielectrophoresis (DEP)*

The electric field gradients in the OET device results in an optically-induced DEP force. This DEP force results from the interaction of a non-uniform electric field and the induced dipole of a particle within the electric field. This force can be described by the following equation, assuming the particle is a homogeneous dielectric sphere:

$$F_{DEP} = 2\pi r^3 \varepsilon_m \,\mathrm{Re}[K(\omega)]\nabla E_{rms}^2 \qquad (1)$$

where $r$ is the particle radius, $\varepsilon_m$ is the permittivity of the medium surrounding the particle, $E_{rms}$ is the root-mean-square electric field strength, and Re[$K(\omega)$] is the real part of the Clausius-Mossotti factor, given by:

$$K(\omega) = \frac{\varepsilon_p^* - \varepsilon_m^*}{\varepsilon_p^* + 2\varepsilon_m^*}, \varepsilon_p^* = \varepsilon_p - j\frac{\sigma_p}{\omega}, \varepsilon_m^* = \varepsilon_m - j\frac{\sigma_m}{\omega} \qquad (2)$$

where $\varepsilon$ is the permittivity of the particle or medium (denoted by a subscript $p$ or $m$), $\sigma$ is the conductivity of the particle or medium, and $\omega$ is the angular frequency of the electric field [6]. Positive values of Re[$K(\omega)$] result in particle attraction to electric field maxima (positive DEP). For negative values of Re[$K(\omega)$], particles are repelled from field maxima (negative DEP). Many cell types are uniquely distinguishable by the real part of the Clausius-Mossotti factor. This enables the separation of different cell types using DEP force.

## III. Cell Trapping and Discrimination

As different cell types exhibit dissimilar electrical properties, DEP can be used to sort between cell types, or even between widely varying cells of the same type [7-9]. This property is useful for cellular manipulation, in which heterogeneous mixtures of cells are common. We use this capability to selectively concentrate live human B cells from dead B cells, and to spatially discriminate a mixed population of Jurkat and HeLa cells.

In a live cell, the semi-permeable phospholipid membrane allows a cell to maintain an ion differential between its interior and the surrounding liquid medium. In these OET experiments, cells are suspended in a low-conductivity isotonic buffer (8.5% sucrose and 0.3% dextrose), so the cells have internal conductivities greater than the liquid. However, once a cell dies, the ion differential is no longer maintained, and the conductivity of the cell interior becomes the same as the surrounding liquid. This means that the Clausius-Mossotti factor is different for live and dead cells (Fig. 2). The simulated results predict that for applied frequencies greater than approximately 60 kHz, live B cells will experience a positive DEP force, while dead B cells will experience a negative DEP force.

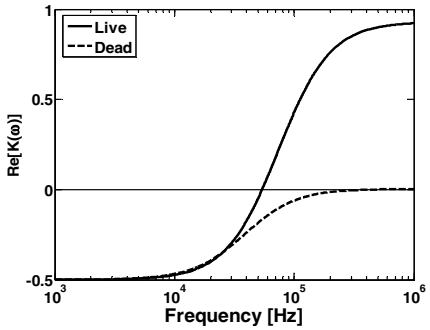


Figure 2. Real part of the Clausius-Mossotti factor for live and dead B cells.

The difference in DEP response between live and dead B cells is used to selectively concentrate live B cells at an applied frequency of 120 kHz [4]. The selective collection pattern is a series of broken concentric rings (Fig. 3). As the concentric rings shrink, the live cells are focused to the center of the pattern by positive DEP. In contrast, the dead cells experience negative DEP, and slip through the gaps in the ring patterns. Trypan blue dye identifies live and dead cells; live cells exclude the dye, and appear clear. The dead cells, which have a permeable membrane, absorb the dye, and appear dark.

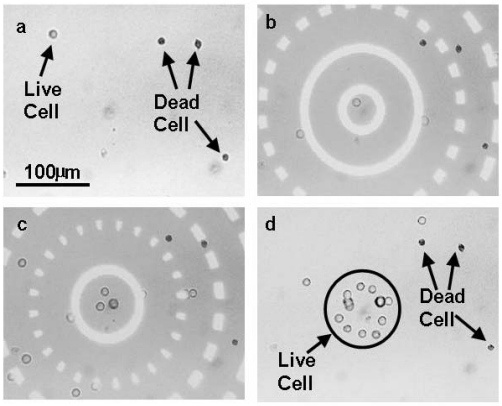


Figure 3. Selective concentration of live B cells from dead B cells. (a) The initial positions of live (clear) and dead (dark) B cells. (b, c) A broken concentric ring pattern is used to transport the live cells to the center of the field of view while leaving the dead cells behind. (d) The live cells have been concentrated to the central region of the optical pattern. From [4].

In addition to differentiating between live and dead cells, OET force can be used to discriminate between different cell types, such as HeLa and Jurkat cells. In order to spatially separate the HeLa and Jurkat cells, a scanning line optical pattern is used to exploit the differences in OET force on the cells [10]. A 15-μm-wide leading line and a 23-μm-wide trailing line are separated by ~40 μm, and are simultaneously scanned at a rate of 13 μm/s. The leading line produces a weaker OET force than the thicker trailing line. Thus, as the two lines are scanned across the OET device, the Jurkat cells, which experience a stronger OET force, are held by the leading line. The leading line does not produce sufficient force to transport the HeLa cells against the viscous drag, which are subsequently attracted to and transported by the trailing line. After the scan is completed, the cells retain a spatial separation

equal to the spacing of the two scanning lines. The results of the optical line scanning on a mixed population of Jurkat and HeLa cells are shown in Figure 4.

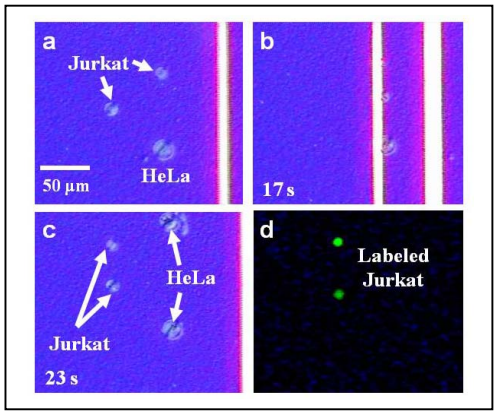


Figure 4. OET-enabled spatial discrimination of live Jurkat and HeLa cells. (a) The initial cell positions before the optical pattern is scanned from right to left across the field-of-view. (b) The cells are attracted to the leading line. The HeLa cell is starting to lag the scanning line. (c) The cells after the scan is completed, showing spatial separation. An additional HeLa cell has moved into the field-of-view during the scan. (d) Fluorescent image of the cells in (c), verifying that the leading cells are the fluorescent-labeled Jurkat cells. From [10].

## IV. Cell Manipulation in Cell Culture Media

Although OET has been used to manipulate a variety of cell types, including red and white blood cells [11], it is limited by the a-Si photoconductive material. The photoconductivity of a-Si allows efficient OET operation only in low-conductivity solutions (less than 0.1 S/m). Thus, low-conductivity isotonic solutions are necessary to facilitate cell manipulation in an OET device. These low-conductivity media are non-physiological, and eventually reduce cell viability. The usage of non-physiological media also limits the use of some reagents, and is undesirable for some biological applications. Thus, we have developed a phototransistor-based OET (Ph-OET) device that enables the manipulation of cells in highly-conductive solutions, such as physiological buffers and cell culture media (Fig. 5) [12].

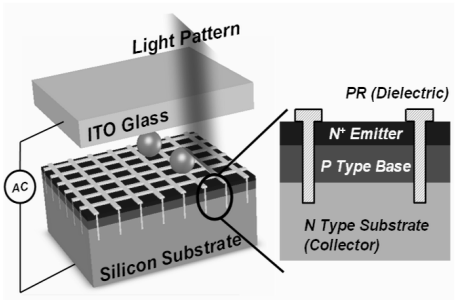


Figure 5. Schematic of phototransistor-based OET device (Ph-OET)

In the Ph-OET device, the a-Si photoconductive layer is replaced by a layer of single-crystalline silicon bipolar phototransistors. Each phototransistor consists of a heavily n-doped emitter (N= $10^{20}$ $cm^{-3}$), a p-doped base (P= $10^{16}$ $cm^{-3}$), and a lightly n-doped collector (N= $6x10^{14}$ $cm^{-3}$). Each vertical phototransistor structure forms 10 µm x 10 µm square pixels. The pixels are isolated by deep-reactive-ion-etched 2-µm-wide trenches. The trenches are filled with an insulating material to avoid direct contact between the liquid and the base area.

The phototransistors offer much higher photoconductivity than the a-Si photoconductor used in conventional OET, thanks to the high carrier mobility and the large current gain (Fig. 6). The phototransistors exhibit a photoconductivity more than 2 orders of magnitude higher than that of a-Si at an optical power density of 1 $W/cm^2$. To operate the OET in physiological solutions with a conductivity of 1.5 S/m, the photoconductivity should be greater than 1.5 $S/cm^2$, assuming a liquid layer thickness of 100 µm. This is satisfied in a Ph-OET device with a light intensity of less than 0.3$W/cm^2$, while a-Si-based OET devices require greater than 50$W/cm^2$. The low optical power requirement of Ph-OET reduces heating and avoids photo-damage of biological samples.

HeLa and Jurkat cells have been successfully manipulated in phosphate-buffered saline (PBS) and Dulbecco's Modified Eagle Medium (DMEM) solutions using the Ph-OET device (Fig. 7). Both solutions have a conductivity of 1.5 S/m. The average cell velocities observed in PBS and DMEM are similar due to their identical conductivity.

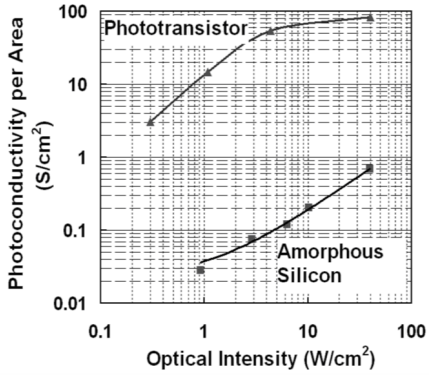


Figure 6. Photoconductivity comparison between the phototransistor and amorphous silicon OET devices

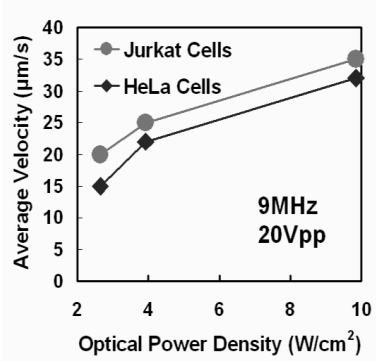


Figure 7. Cell velocity as a function of optical intensity. Cells are suspended in PBS and manipulated using the Ph-OET device.

## V. Nanowire Patterning and Assembly

OET forces are also capable of acting on nanoscale structures, such as nanowires. Elongated structures such as nanowires experience a torque in addition to the DEP force, which aligns the dipole of the nanowire so that it is parallel to the electric field. Thus, the major axis of nanowires in the OET device is perpendicular to the surface of the OET device. (Fig. 8a) [13]. Maximum trapping speeds for an individual silicon nanowire with 100 nm diameter and 5 μm length approach 135 μm/s using an ac bias 20 Vpp at 100 kHz. This is approximately 4 times the maximum speed achievable by optical tweezers [14], and is reached with 5 to 6 orders of magnitude less optical intensity than with optical tweezers.

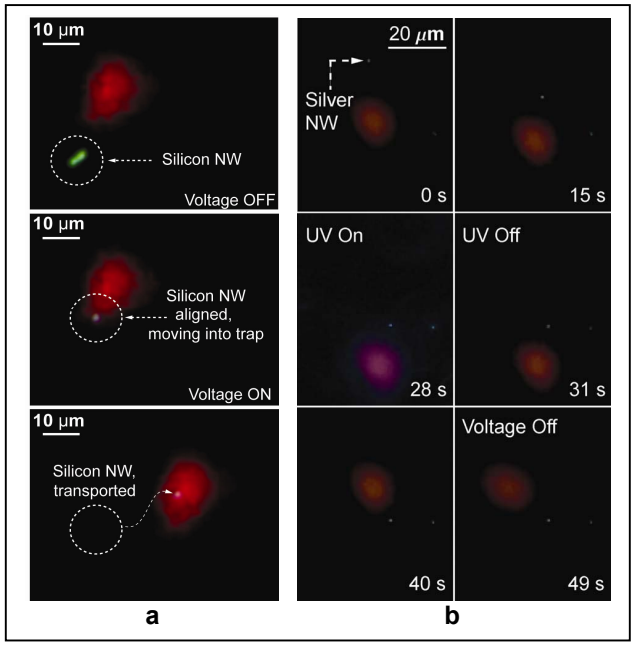


Figure 8. (a)Trapping of an individual silicon nanowire using a laser spot. (Top) No voltage is applied across the device, and the nanowire undergoes Brownian motion. (Middle) voltage is applied, the long-axis of the nanowire aligns with the electric field and the nanowire moves into the trap. (Bottom) The nanowire follows the laser trap position. (b) In-situ trapping and immobilization of an individual silver nanowire in a a poly(ethylene glycol) diacrylate (PEGDA) photocurable polymer solution. Once the nanowire is positioned at the desired location, the manipulation area is exposed to a UV source, polymerizing the hydrogel solution and fixing the wire in place. After polymerization, the nanowire's position and orientation remain stable. From [13].

It is possible to preserve the position and orientation of the wires trapped with OET using a photocurable polymer solution such as PEGDA (Fig. 8b) [15]. This enables subsequent post-processing steps, such as the deposition of metallic contacts for the formation of nanowire sensors.

## VI. Conclusion

Optoelectronic tweezers is a versatile platform that enables single-cell manipulation and nanowire assembly on the same platform. OET manipulation can aid cellular-level diagnostics by positioning, sorting, and patterning cells at the single-cell level. In addition, OET also enables the assembly of nanowire sensors, and allows the controlled positioning of single nanowires for use as cellular probes.

## Acknowledgment

These projects have been funded by the Center for Cell Control (CCC), a NIH Nanomedicine Center, and by the Institute for Cell Mimetic Space Exploration (CMISE), a NASA URETI. The authors would like to thank the UC Berkeley Tissue Culture Facility for providing cells, and Peidong Yang's research group at UC Berkeley for providing silicon and silver nanowires.

## References

[1] D. G. Grier, "A revolution in optical manipulation," *Nature,* vol. 424, pp. 810-816, Aug 14 2003.

[2] J. Voldman, "Electrical forces for microscale cell manipulation," *Annual Review Of Biomedical Engineering,* vol. 8, pp. 425-454, 2006.

[3] S. K. Mohanty, A. Rapp, S. Monajembashi, P. K. Gupta, and K. O. Greulich, "Comet assay measurements of DNA damage in cells by laser microbeams and trapping beams with wavelengths spanning a range of 308 nm to 1064 nm," *Radiation Research,* vol. 157, pp. 378-385, Apr 2002.

[4] P. Y. Chiou, A. T. Ohta, and M. C. Wu, "Massively parallel manipulation of single cells and microparticles using optical images," *Nature,* vol. 436, pp. 370-372, Jul 21 2005.

[5] R. Schwarz, F. Wang, and M. Reissner, "Fermi level dependence of the ambipolar diffusion length in silicon thin film transistors," *Applied Physics Letters,* vol. 63, pp. 1083-5, 1993.

[6] T. B. Jones, *Electromechanics of Particles*. Cambridge: Cambridge University Press, 1995.

[7] P. R. C. Gascoyne, X.-B. Wang, Y. Huang, and F. F. Becker, "Dielectrophoretic separation of cancer cells from blood," *IEEE Transactions on Industry Applications,* vol. 33, pp. 670-8, 1997.

[8] R. Pethig, M. S. Talary, and R. S. Lee, "Enhancing traveling-wave dielectrophoresis with signal superposition," *IEEE Engineering In Medicine And Biology Magazine,* vol. 22, pp. 43-50, Nov-Dec 2003.

[9] P. R. C. Gascoyne and J. V. Vykoukal, "Dielectrophoresis-based sample handling in general-purpose programmable diagnostic instruments," *Proceedings Of The IEEE,* vol. 92, pp. 22-42, Jan 2004.

[10] A. T. Ohta, P.-Y. Chiou, H. L. Phan, S. W. Sherwood, J. M. Yang, A. N. K. Lau, H.-Y. Hsu, A. Jamshidi, and M. C. Wu, "Optically Controlled Cell Discrimination and Trapping Using Optoelectronic Tweezers," *Selected Topics in Quantum Electronics, IEEE Journal of,* vol. 13, pp. 235-243, 2007.

[11] A. T. Ohta, P. Y. Chiou, T. H. Han, J. C. Liao, U. Bhardwaj, E. R. B. McCabe, F. Yu, R. Sun, and M. C. Wu, "Dynamic Cell and Microparticle Control via Optoelectronic Tweezers," *Microelectromechanical Systems, Journal of,* vol. 16, pp. 491-499, 2007.

[12] H. Y. Hsu, A. T. Ohta, P. Y. Chiou, A. Jamshidi, and M. C. Wu, "Phototransistor-based optoelectronic tweezers for cell manipulation in highly conductive solution," in *Transducers '07 & Eurosensors XXI: 14th International Conference on Solid-State Sensors, Actuators and Microsystems*, Lyon, France, 2007, pp. 477-480.

[13] A. Jamshidi, P. J. Pauzauskie, P. J. Schuck, A. T. Ohta, P. Y. Chiou, J. Chou, P. D. Yang, and M. C. Wu, "Dynamic manipulation and separation of individual semiconducting and metallic nanowires," *Nature Photonics,* vol. 2, pp. 85-89, Feb 2008.

[14] P. J. Pauzauskie, A. Radenovic, E. Trepagnier, H. Shroff, P. Yang, and J. Liphardt, "Optical trapping and integration of semiconductor nanowire assemblies in water," *Nat Mater,* vol. 5, pp. 97-101, 2006.

[15] D. R. Albrecht, V. L. Tsang, R. L. Sah, and S. N. Bhatia, "Photo- and electropatterning of hydrogel-encapsulated living cell arrays," *Lab on a Chip,* vol. 5, pp. 111-118, 2005.